# Electrochemical Deposition of Nanostructured ($H_1$-e) Layers of Two Metals in Which Pores within the Two Layers Interconnect

P. N. Bartlett* and J. Marwan

*Department of Chemistry, University of Southampton, Southampton, SO17 1BJ, United Kingdom*

*Received October 22, 2002. Revised Manuscript Received March 6, 2003*

Electrochemical deposition of metals from the $H_1$ hexagonal phase of nonionic lyotropic liquid-crystalline phases has been shown to produce films which contain regular arrays of uniform pores whose dimensions are determined by those of the micelles in the lyotropic phase used as the template. In this paper we report results for a study of the deposition of one $H_1$-e metal film on top of another. Using $H_1$-e films of palladium and rhodium as a model system we show, using electrochemical measurements, that the surface of the pores of the inner metal film are not blocked by deposition of an overlayer of the second mesoporous metal. By studying the evolution of the voltammetry of the mesoporous metallic bilayers as the surfactant is leached out of the pores over time, we conclude that the pores in the outer $H_1$-e metal film connect to those in the inner layer so that we have a hexagonal array of continuous pores running though both metal layers in the structure.

## Introduction

In a number of papers published over the last 5 years we have shown that we can electrochemically deposit a range of metals with regular mesoporous architectures by using lyotropic liquid-crystalline phases as templates.[1−5] In this paper we extend this idea and demonstrate that we can electrochemically deposit mesoporous films of two metals, one on top of the other, in such a way that we produce a single nanostructure in which the pores run continuously through the two metal layers.

The idea of using the lyotropic liquid-crystalline phases of nonionic surfactants to template the deposition of inorganic materials was first introduced by Attard who demonstrated the formation of nanostructured silica by hydrolysis of tetramethyl orthosilicate[6] and platinum by chemical reduction of hexachloroplatinic acid.[7] In this approach a high concentration of the nonionic surfactant, typically 40−60 wt %, is employed and the nanostructure is a direct cast of the structure of the lyotropic phase used to template the deposition. Although different lyotropic phases can be used as templates, including the cubic *Ia*3*d* and lamellar phases, the hexagonal $H_1$ phase is the most widely reported. In the hexagonal phase the surfactant molecules assemble into long cylindrical micelles and these micelles then pack into a hexagonal array in which the separation between the micelles is comparable to their diameter (around 2 nm).[8] When these phases are used to template the electrochemical deposition of metal films, the metal salt and electrolyte are dissolved into the aqueous component of the mixture and metal deposition occurs, out from the electrode surface, around the surfactant micelles, Figure 1. Once deposition is complete, the surfactant is removed by washing to leave a metal film punctured by a regular hexagonal array of uniform pores. The thickness of the film is directly controlled by the total charge passed. The resulting nanostructured films are denoted as $H_1$-e films to indicate their regular nanoarchitecture and the topology of the pores within the structure.

The use of this template deposition technique allows considerable control over the structure of the mesoporous film. For example, by changing the surfactant used for platinum deposition from octaethyleneglycol monohexadecyl ether ($C_{16}EO_8$) to octaethyleneglycol monododecyl ether ($C_{12}EO_8$), it is possible to change both the diameter of the pores and the thickness of the metal walls between them from 2.5 to 1.7 nm.[1] On the other hand, by adding an organic cosolvent, such as heptane, to the $C_{16}EO_8$ plating mixture, it is possible to swell the surfactant micelles without changing their separation and thus increase the diameter of the pores in the platinum film to 3.5 nm while leaving the thickness of the walls the same.[1]

$H_1$-e metal films have very high surface areas (in excess of $10^6$ $cm^2$ $cm^{-3}$) and have been shown to be

(1) Attard, G. S.; Bartlett, P. N.; Coleman, N. R. B.; Elliott, J. M.; Owen, J. R.; Wang, J. H. *Science* **1997**, *278*, 838−840.
(2) Bartlett, P. N.; Birkin, P. R.; Ghanem, M. A.; de Groot, P.; Sawicki, M. *J. Electrochem. Soc.* **2001**, *148*, C119−C123.
(3) Bartlett, P. N.; Gollas, B.; Guerin, S.; Marwan, J. *Phys. Chem. Chem. Phys.* **2002**, *4*, 3835−3842.
(4) Elliott, J. M.; Birkin, P. R.; Bartlett, P. N.; Attard, G. S. *Langmuir* **1999**, *15*, 7411−7415.
(5) Elliott, J. M.; Attard, G. S.; Bartlett, P. N.; Coleman, N. R. B.; Merckel, D. A. S.; Owen, J. R. *Chem. Mater.* **1999**, *11*, 3602−3609.
(6) Attard, G. S.; Glyde, J. C.; Goeltner, C. G. *Nature* **1995**, *378*, 366−368.
(7) Attard, G. S.; Goeltner, C. G.; Corker, J. M.; Henke, S.; Templer, R. H. *Angew. Chem., Int. Ed. Engl.* **1997**, *36*, 1315−1317.
(8) Mitchell, D. J.; Tiddy, G. J. T.; Waring, J.; Bostock, T.; McDonald, M. P. *J. Chem. Soc., Faraday Trans. 1* **1983**, *79*, 975−1000.

10.1021/cm0210400 CCC: $25.00 
Published on Web 06/18/2003

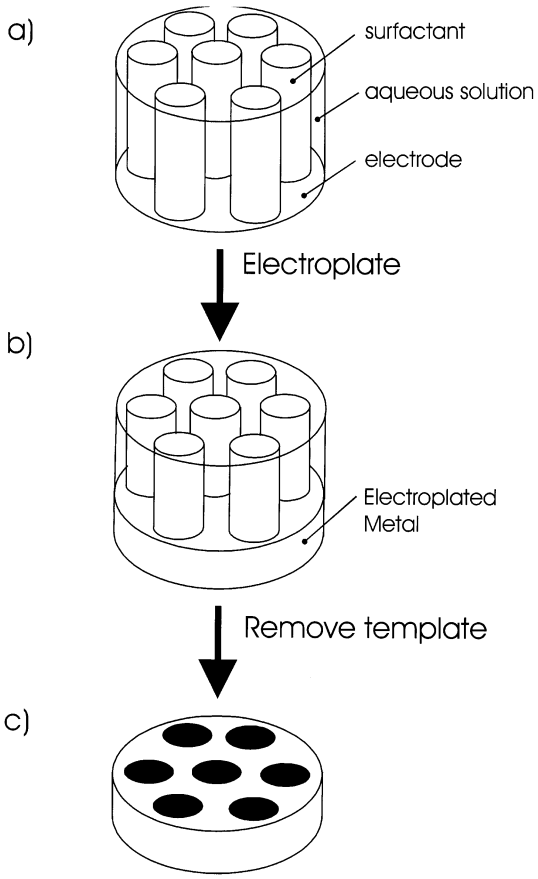


**Figure 1.** Schematic representation of the templating process used to deposit the $H_1$-e films. The cylinders represent the micellar rods in the lyotropic liquid-crystalline phase.

useful catalysts in electroanalysis[4,9,10] and in chemical sensors[11] and to have potential applications in batteries[12] and fuel cells.[13] In this paper we show that we can deposit one $H_1$-e film on top of another in such a way that the pores within the two films interconnect. This opens up the possibility of fabrication of mesoporous multilayers which may have interesting catalytic, or other, properties.

To demonstrate the deposition of two $H_1$-e films in such a way that the hexagonal array of pores runs continuously through the final film, we use cyclic voltammetric measurements. The voltammetry of noble metals such as platinum, palladium, and rhodium in acid solutions is characterized by reasonably well understood surface reactions corresponding to the formation and stripping of oxide films or adsorbed hydrogen films at the metal surface.[14] These processes occur at potentials which are characteristic of the different metals, and which are distinguishable from those for alloys of the metals.[15] In addition, the formation of adsorbed hydrogen, or of surface oxide layers, is associated with the passage of a fixed amount of charge for each metal atom at the surface so that the charge passed in these processes can be used to determine the electroactive surface area of the metal.[16] Thus, by selecting a pair of noble metals for which the oxide stripping peaks occur at well-separated potentials, we can use the charge passed in the oxide stripping to directly measure the area of the metal in direct contact with the electrolyte solution. Using this approach, for our bilayer system, we can simultaneously determine the areas of the upper and lower layer which contact the electrolyte. If the pores in the two layers connect, then we should see voltammetry for the lower metal layer even in the presence of a continuous overlayer. If the pores do not connect, then the voltammetry of the lower layer will be suppressed. Although this method is not as direct as, for example, using transmission electron microscopy, it is highly sensitive, it provides quantitative information about the electroactive surface area of the two metals, and it samples the whole of the structure. Using a technique such as TEM to study these films is very difficult because the pores are small (around 3-nm diameter), the interface between the two metals is buried within the film, the contrast in the image between the two metals is poor, and the TEM technique can only image a very small part of the whole structure. Thus, while the TEM images confirm the presence of the expected $H_1$ nanostructure, they do not provide direct evidence for the communication between the pores in the two layers.

## Experimental Section

**Experimental.** Hydrochloric acid (AnalaR BDH), sulfuric acid (AnalaR BDH), ammonium tetrachloropalladate (premion-99.998% Alfa Aesar), hydrogen hexachloroplatinate(IV) hydrate (99.9% Aldrich), rhodium(III) chloride (99.9% Alfa Aesar), octaethyleneglycol monohexadecyl ether ($C_{16}EO_8$, Fluka), and heptane (99%, Lancaster) were all used as-received. All aqueous solutions were freshly prepared using reagent-grade water (18 MΩ-cm) from a Whatman "Stillplus" system coupled to a Whatman RO 50. All glassware were soaked overnight in a 3% Decon/deionized water solution and washed thoroughly at least three times with deionized water prior to use.

All electrochemical experiments were carried out using an EG&G Model 263A potentiostat/galvanostat with a large area platinum gauze counter electrode and either a homemade saturated mercury sulfate reference electrode (SMSE) or saturated calomel electrode (SCE). The counter electrode was a large area platinum gauze. The SMSE was used to avoid chloride contamination of the sulfuric acid electrolyte solution used in the studies of the nanostructured metal electrodes and all potentials are reported with respect to this reference electrode (potentials with respect to SMSE are shifted 0.45 V negative of the corresponding potential vs SCE). The reference electrode was used in conjunction with a luggin capillary and stored in a saturated potassium sulfate solution when not in use.

The phase of the lyotropic liquid-crystalline plating mixtures was confirmed by polarized light microscopy using an Olympus BH-2 polarized light microscope equipped with a Linkam TMS90 heating stage and temperature control unit. Phases were assigned on the basis of their characteristic optical textures.[8]

(9) Evans, S. A. G.; Elliott, J. M.; Andrews, L. M.; Bartlett, P. N.; Doyle, P. J.; Denuault, G. *Anal. Chem.* **2002**, *74*, 1322−1326.

(10) Birkin, P. R.; Elliott, J. M.; Watson, Y. E. *J. Chem. Soc., Chem. Commun.* **2000**, 1693.

(11) Bartlett, P. N.; Guerin, S.; Marwan, J.; Gardner, J. W.; Lee, S. M.; Willett, M. J.; Leclerc, S. A. A. In *Symposium on Microfabricated Systems and MEMS−V*; The Electrochemical Society: Philadelphia, 2002.

(12) Whitehead, A. H.; Elliott, J. M.; Owen, J. R. *J. Power Sources* **1999**, *81−82*, 33−38.

(13) Jiang, J.; Kucernak, A. *J. Electroanal. Chem.* **2002**, *520*, 64−70.

(14) Sawyer, D. T.; Roberts, J. L. *Experimental Electrochemistry for Chemists*; Wiley-Interscience: New York, 1974.

(15) Rand, D. A. J.; Woods, R. *J. Electroanal. Chem.* **1972**, *36*, 57−68.

(16) Rand, D. A. J.; Woods, R. *J. Electroanal. Chem.* **1970**, *31*, 29−38.

The $H_I$-e metal films were freshly prepared before each electrochemical experiment by electrochemical deposition on to gold disk electrodes (area 0.0079 $cm^2$) formed by sealing 1 ± 0.1 mm diameter gold wire in glass. Immediately before use, the gold disk electrodes were freshly polished using silicon carbide paper (Cc 1200, English Abrasives) and then alumina/water slurries (Beuhler) starting with a particle size of 25 $\mu$m and ending with a particles size of 0.3 $\mu$m. $H_I$-e metal films were deposited from a solution containing 12 wt % $(NH_4)_2PdCl_4$ or $RhCl_3$, 47 wt % $C_{16}EO_8$, 39 wt % water, and 2 wt % heptane at 25 °C. These conditions correspond to the hexagonal ($H_1$) lyotropic phase for both mixtures as determined by studies of the phase diagram for the system.[3] These deposition mixtures are highly viscous and must be prepared with care to ensure a uniform composition. After all of the components were mixed, the mixture was heated and stirred to ensure homogeneity and then cooled before use.

Palladium was deposited from the liquid-crystalline plating mixture at 0.1 V and rhodium at −0.2 V vs SCE. The total amounts of the metals deposited, assuming 100% faradaic efficiency for the process, were controlled by controlling the total amount of charge passed and was usually 0.44 C $cm^{-2}$ corresponding, respectively, to the deposition of 1.9 $\mu$g for palladium or 1.2 $\mu$g for rhodium onto the electrodes. The deposition took typically 150 s for the thinnest films. After deposition the $H_1$-e metal films were rinsed in purified water to remove the adhering surfactant mixture.

Electrochemical measurements on the $H_I$-e metal films were carried out at room temperature (18−23 °C) in 1 M $H_2SO_4$. Before each experiment the solution was sparged for 10−15 min with a stream of highly purified argon gas to displace dissolved oxygen. The electrochemically active surface areas of the $H_1$-e metal films were estimated by integrating the charge passed in the surface oxide stripping reaction recorded in 1 M sulfuric acid following the procedure suggested by Rand and Woods.[16] SEM studies showed that these deposition conditions produced smooth continuous films of both metals.

SEM and TEM images were obtained using a Philips XL30ESEM and a JEOL 2000FX transmission electron microscope operating at an accelerating voltage of 200 kV, respectively. The samples for TEM characterization were prepared by scratching small particles of the film onto a Cu TEM grid using a scalpel.

## Results and Analysis

The two noble metals which we chose to use for these experiments were palladium and rhodium because they have very characteristic voltammetry in acid solution with well-separated oxide stripping peaks, because we have already characterized the $H_1$-e films for these two metals and because we can deposit smooth continuous films of both. Figure 2 shows a typical cyclic voltammogram for an $H_1$-e Pd film deposited from a $C_{16}EO_8$ template mixture.[3] Formation of the surface oxide starts at around 0.07 V on the anodic sweep and shows two peaks at 0.22 and 0.41 V. On the return cycle the surface oxide is removed at 0.02 V. The same voltammetry is seen for ordinary palladium electrodes and has been studied in some detail.[17] On continuing the cathodic scan, we see the formation of adsorbed hydrogen at −0.46 V followed by formation of the alpha hydride around −0.53 V and then the onset of beta hydride formation at the cathodic limit. These processes are reversed as the potential starts to scan anodic again. The voltammetry of the $H_1$-e palladium electrode at cathodic potentials is different from that of ordinary palladium electrodes but resembles that reported for

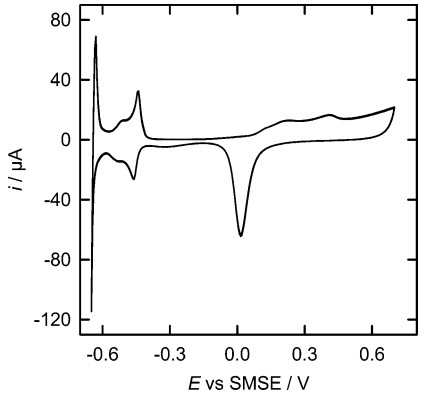


**Figure 2.** Cyclic voltammogram of an $H_1$-e Pd film (200-nm thick, deposited from a plating mixture of 12 wt % $(NH_4)_2PdCl_4$, 47 wt % $C_{16}EO_8$, 39 wt % water, and 2 wt % heptane on a gold disk electrode, area 0.0079 $cm^2$, total deposition charge 3.5 mC) recorded at 20 mV/s in 1 M sulfuric acid. The film was soaked in water for 1 h before the start of the voltammetry to remove all surfactant from the pores.

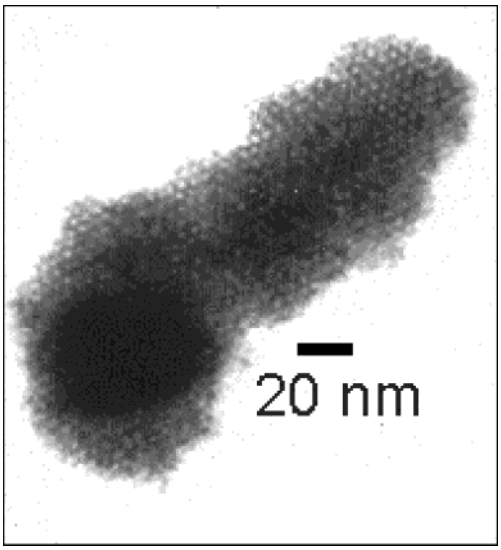


**Figure 3.** TEM of a sample of $H_1$-e palladium.

nanoparticulate palladium. This is because the high surface area of the metal combined with the thin palladium walls between the pores means that the processes corresponding to the formation of adsorbed and absorbed hydrogen are particularly well-resolved.[3] The structure of these films has been confirmed by small-angle X-ray reflection and transmission electron microscopy and a full description of this together with discussion of the voltammetry of the $H_1$-e palladium electrode in acid are given in the literature.[3] Figure 3 shows a TEM image of the nanostructured Pd film. The regular hexagonal arrangement of the pores within the metal is clearly shown. On the basis of these and other TEM measurements, we find that the diameter of the pores is around 3 nm with a pore center to pore center separation of around 6 nm. From the voltammetry in Figure 2, we can estimate the electroactive surface area of the palladium film by integrating the charge passed to remove the surface oxide film. Using this charge together with the value given by Rand and Woods[16] for oxide stripping on palladium of 424 $\mu$C $cm^{-2}$, we obtain an area of 0.76 $cm^2$. Then taking into account the total charge passed to deposit the film, we calculate a specific surface area for this palladium film of 39 $m^2$ $g^{-1}$

(17) Burke, L. D.; Casey, J. K. *J. Electrochem. Soc.* **1993**, *140*, 1284−1291.

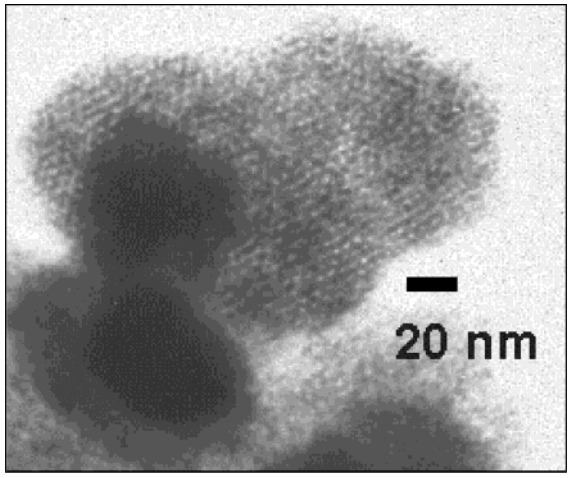


**Figure 4.** TEM of a sample of $H_1$-e rhodium.

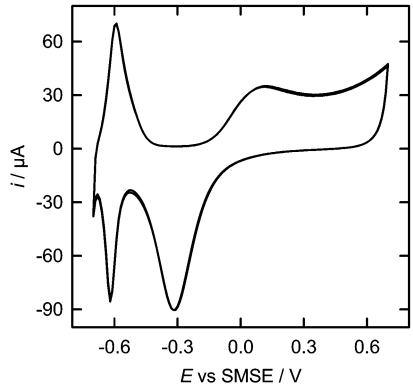


**Figure 5.** Cyclic voltammogram of an $H_1$-e Rh film (126-nm thick, deposited from a plating mixture of 12 wt % $RhCl_3$, 47 wt % $C_{16}EO_8$, 39 wt % water, and 2 wt % heptane on a gold disk electrode, area 0.0079 $cm^2$, total deposition charge 3.5 mC) recorded at 50 mV/s in 1 M sulfuric acid. The film was soaked in water for 1 h prior to the voltammetry to remove all surfactant from the pores.

corresponding to $4.7 \times 10^6$ $cm^2$ $cm^{-3}$, a value which is consistent with the film's $H_1$ nanostructure.

Figure 4 shows a TEM image for an $H_1$-e rhodium film. Again, the expected regular hexagonal nanostructure is clearly seen with a pore diameter of around 3 nm and a pore center to pore center separation of around 6 nm. Full details of the deposition and characterization of these films, including small-angle X-ray and TEM studies, are given elsewhere.[18] Figure 5 shows the corresponding voltammogram for the film. For the $H_1$-e rhodium electrode oxide formation starts at around −0.16 V on the anodic scan and the current passes through a peak at 0.11 V. On the return scan the oxide film is stripped from the electrode at −0.31 V. This is followed, at more cathodic potentials, by formation of adsorbed hydrogen at −0.61 V. The adsorbed hydrogen is removed from the electrode surface on the anodic sweep at −0.59 V. The voltammetry observed for the $H_1$-e rhodium electrode is very similar to that reported in the literature for ordinary polycrystalline rhodium electrodes.[19] Using the conversion factor of 660 $\mu$C $cm^{-2}$ for oxide stripping on rhodium given by Jerkiewicz and

(18) Bartlett, P. N.; Marwan, J. *Microporous Mesoporous Mater.*, submitted.

(19) Jerkiewicz, G.; Borodzinski, J. J. *Langmuir* **1993**, *9*, 2202.

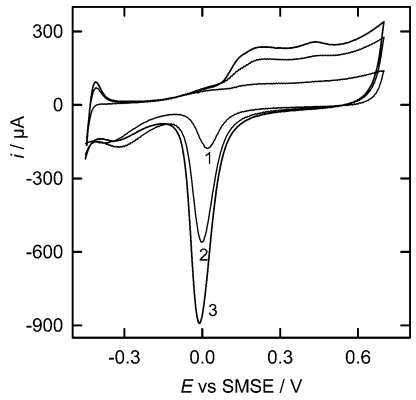


**Figure 6.** Cyclic voltammograms recorded at 100 mV/s in 1 M $H_2SO_4$ for three different films with $H_1$-e Pd deposited on top of $H_1$-e Rh on a gold disk electrode (area 0.0079 $cm^2$). In each case the charge passed for $H_1$-e Rh deposition was kept constant at 3.5 mC while the amount of charge passed for $H_1$-e Pd deposition was increased from (1) 3.5 to (2) 7.0 mC and then (3) 10.5 mC.

Borodzinski,[19] we obtain a surface area of 0.40 $cm^2$ by integrating the charge under the oxide stripping peak in Figure 5. With use of the known deposition charge for the film, this gives an estimated specific area for the film of 33 $m^2$ $g^{-2}$ corresponding to $4.1 \times 10^6$ $cm^2$ $cm^{-3}$, which is consistent with the $H_1$ structure of the film.

Comparing Figures 2 and 5, we can see that the oxide stripping peaks for the two metals are well-separated and should, therefore, be easily distinguishable in the voltammetry of a bilayer film in which both metals are exposed to the solution.

Figure 6 shows a set of voltammograms for three bilayer films which were prepared by first depositing a film of $H_1$-e rhodium approximately 126-nm thick (as determined from the deposition charge used) and then covering this with films of $H_1$-e palladium of different thicknesses. In doing these experiments, we were obviously concerned about the choice of deposition conditions required to achieve communication between the pores in the two mesoporous layers of the film. First, we were careful to use the same surfactant and concentration of cosolvent to prepare the plating mixtures since we know that these alter the dimensions of the nanostructure. We also gave some thought to the treatment of the electrode between deposition of the first and second layers. In the experiments shown, the electrode was washed superficially to remove the rhodium plating mixture from the surface before placing in the palladium plating solution. Since we know from other experiments[3] that it is necessary to wash the $H_1$-e films for at least several minutes to remove all the surfactant from the pores, we assume that this superficial washing leaves the pores of the rhodium film filled by $C_{16}EO_8$ when it is transferred to the palladium plating solution and we reasoned that this might be important for achieving communication between the pores in the two layers. However, in separate experiments in which the $H_1$-e film deposited first was washed extensively to remove all the surfactant before placing in the second plating mixture, we obtain identical results so that we believe that the precise details of the washing of the films between deposition steps are not important. After deposition of the top $H_1$-e palladium film, the electrode was extensively washed to remove all the surfactant and

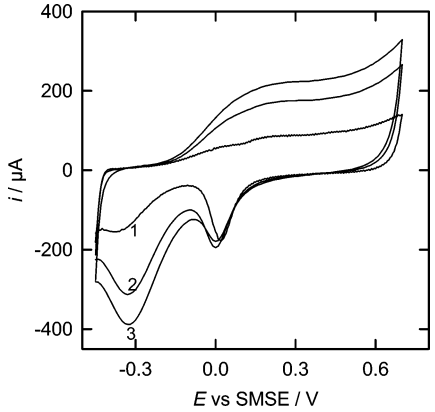


**Figure 7.** Cyclic voltammograms recorded at 100 mV/s in 1 M $H_2SO_4$ for three different films with $H_1$-e Rh deposited on top of $H_1$-e Pd on a gold disk electrode (area 0.0079 $cm^2$). In each case the charge passed for $H_1$-e Pd deposition was kept constant at 3.5 mC while the amount of charge passed for $H_1$-e Rh deposition was increased from (1) 3.5 to (2) 7.0 mC and then to (3) 10.5 mC.

then the voltammograms shown in Figure 6 were recorded. Comparing Figure 6 to Figures 2 and 5, we can see that the bilayer film shows a superposition of the voltammetric features for the palladium and rhodium electrodes. Note, if there were extensive alloying of the rhodium and palladium, then we would expect to see a single-oxide stripping peak at an intermediate potential for that of the two separate metals.[15] In particular, in Figure 6 we can see two peaks (at 0.22 and 0.43 V) and a shoulder (at 0.15 V) on the anodic scan corresponding to oxide formation and two stripping peaks (at 0.0 and −0.33 V assigned to stripping of the palladium and rhodium oxides, respectively) on the return cathodic scan. As the thickness of the outer $H_1$-e palladium film increases from 200 to 400 nm and then 600 nm (as determined by the deposition charge), the stripping peak for palladium oxide at around 0.0 V grows in size, as expected. In contrast, the charge associated with the rhodium oxide stripping peak at −0.33 V remains approximately constant as the thickness of the palladium overlayer increases, clearly indicating that the presence of the $H_1$-e palladium film is not blocking access to the rhodium electrode surface, even though the film is deposited directly on top of the rhodium layer. It is worth pointing out that SEM studies of these films show a smooth continuous layer; there is no evidence of patchy or discontinuous deposition of the metal. By integrating the charges associated with the oxide stripping processes for the rhodium and palladium, we can estimate the electroactive areas of the two layers. From the rhodium oxide stripping peak, we estimate electroactive surface areas of 0.30 $cm^2$ corresponding to a specific surface area for the films of 25 $m^2\ g^{-1}$. This value is comparable to that for the bare $H_1$-e rhodium film without the palladium overlayer, again showing that the $H_1$-e palladium layer does not significantly block the electrolyte access to the pores in the rhodium film.

This same experiment can be carried out with the two layers in the reverse order. Figure 7 shows voltammograms for three films in which a 200-nm-thick film of $H_1$-e palladium was coated by $H_1$-e films of rhodium of three different thicknesses (130, 250, and 380 nm). Again, we see the same features for the formation and

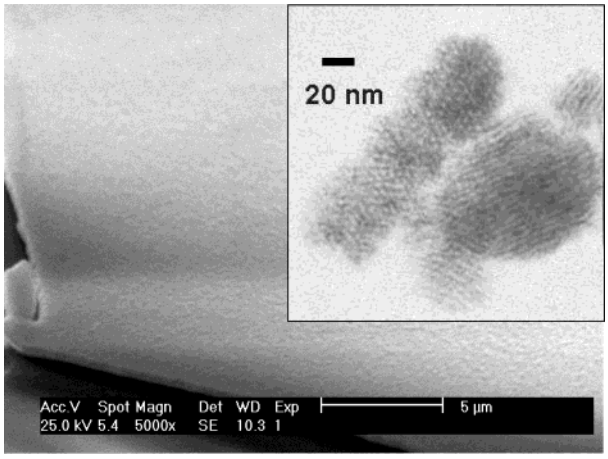


**Figure 8.** SEM and TEM images for a bilayer film of $H_1$-e rhodium (deposition charge 0.42 C/$cm^2$) on $H_1$-e palladium (deposition charge 0.56 C/$cm^2$). The SEM image was obtained at a tilt angle of 70° and shows part of the edge of the film.

stripping of the oxide layers. This time, as expected, the charge for the rhodium oxide stripping at around −0.3 V grows as the rhodium film thickness grows while the charge for the stripping of the palladium oxide film at around 0.0 V stays constant, even though the thickness of the rhodium overlayer is increasing. Integration of the oxide stripping charges for the rhodium and palladium give specific surface areas for the two layers of 22 and 31 $m^2\ g^{-1}$, respectively, values which are consistent with accessible $H_1$ structures for the two layers.

It is important to stress that the mesoporous films are both smooth and continuous and that the metal in the films has the expected nanostructure. Figure 8 shows a composite of SEM and TEM images of one of the rhodium on palladium films. TEM images of the bilayer films confirm the presence of the expected $H_1$ nanostructure, although they are not able to distinguish between rhodium or palladium or demonstrate the connection between the pores in the two metals.The experiments described so far show that when we deposit one $H_1$-e film on top of another, there is no appreciable blocking of the electroactive surface of the lower $H_1$-e film even as the thickness of the top film increases. Clearly this is consistent with continuity between the pores in the lower layer and those in the top layer and is quite difficult to explain in any other way but it is not conclusive proof. Therefore, we carried out further experiments in which we studied the evolution of the voltammetry of the bilayer film after it was transferred directly to the acid solution following only a superficial washing to remove the plating mixture adhering to the outside of the film. We already know from other studies that the pores within the film are filled by surfactant during the deposition and that it takes some time, of the order of minutes, for this surfactant to be leached out of the film when placed in contact with water. Therefore, by superficially washing the film, transferring to the acid solution, and running successive voltammograms, we should see the oxide stripping peaks grow in as the surfactant leaves the pores within the film and the area accessible to the electrolyte, and hence the electroactive area, increases. If the pores running through our metallic bilayer are continuous, we should see the oxide stripping peak for the outer metal layer

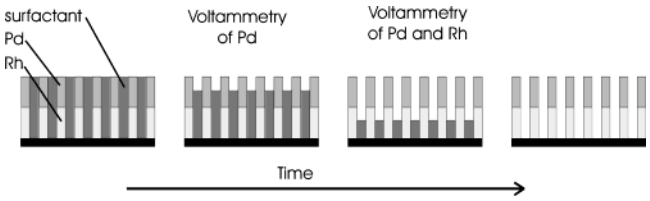


**Figure 9.** Schematic representation of the progressive leaching of surfactant from the pores of the $H_1$-e bilayer.

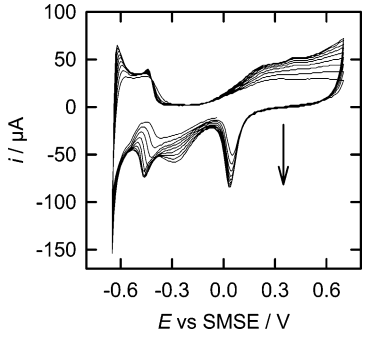


**Figure 10.** Set of cyclic voltammograms recorded at 50 mV/s in 1 M $H_2SO_4$ showing the first 10 cycles for a $H_1$-e Pd film (deposition charge 3.5 mC) deposited on top of an $H_1$-e Rh film (deposition charge 3.5 mC) on a gold disk electrode (area 0.0079 $cm^2$). The bilayer metal film was not soaked in water after deposition.

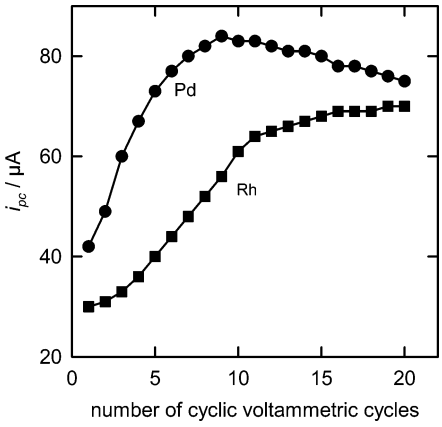


**Figure 11.** Plot of the oxide stripping peak currents for Pd (●, measured at 0.0 V) and Rh (■, measured at −0.3 V) for a bilayer film of $H_1$-e Pd (deposition charge 3.5 mC) deposited on top of $H_1$-e Rh (deposition charge 3.5 mC) on a gold electrode (area 0.0079 $cm^2$) as a function of cycle number. The bilayer film was transferred directly to 1 M $H_2SO_4$ from the plating bath, without first soaking in water, and then cycled at 50 mV/s vs SMSE between −0.45 and 0.7 V.

appear and increase first followed by that for the inner layer, Figure 9, and this will provide conclusive evidence for the continuity of the pores through the film.

Figure 10 shows the first 10 voltammetric cycles after transferring to the acid solution for a 200-nm-thick $H_1$-e palladium film deposited on top of a 126-nm-thick $H_1$-e rhodium film. We can see that the palladium oxide stripping peak at around 0.0 V is clearly visible from the start and increases in size with each cycle. In contrast, the stripping peak for the rhodium oxide at −0.3 V is not clearly resolved in the first voltammogram and grows in more slowly, only becoming clear in the last couple of cycles. Figure 11 shows a plot of the peak cathodic currents at 0.0 and −0.3 V, corresponding to

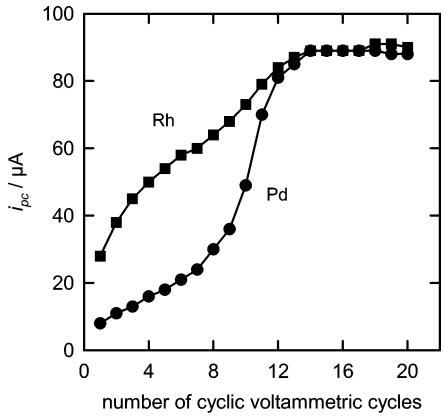


**Figure 12.** Plot of the oxide stripping peak currents for Pd (●, measured at 0.0 V) and Rh (■, measured at −0.3 V) for a bilayer film of $H_1$-e Rh (deposition charge 3.5 mC) deposited on top of $H_1$-e Pd (deposition charge 3.5 mC) on a gold electrode (area 0.0079 $cm^2$) as a function of cycle number. The bilayer film was transferred directly to 1 M $H_2SO_4$ from the plating bath, without first soaking in water, and then cycled at 50 mV/s vs SMSE between −0.45 and 0.7 V.

the two oxide stripping processes, as a function of cycle number. Note that the peak currents have not been corrected for the baseline double-layer charging current so the peak currents measured at 0.0 and −0.3 V have contributions from the oxide stripping of one metal and the double-layer charging of the other. Nevertheless, it is clear from the plot that the oxide stripping peak for the outer, palladium, layer increases before that for the inner, rhodium, layer but that they both eventually reach a plateau when all the surfactant has left the pores. We attribute the slow decrease in the peak current for the palladium oxide at higher cycle number to some dissolution of metal during the experiment.[3] If we integrate the charges for the two stripping peaks at the end of the experiment, we again find high specific surface areas, as we would expect for $H_1$-e films of the two metals.

When we carry out the experiment the other way round with the palladium film on the inside and the rhodium film on the outside, we find that the pattern of increase of the two peak currents with cycle number is reversed, Figure 12. Now the oxide stripping peak for the outer, rhodium, layer grows in first, followed by that for the inner, palladium, layer. Note that the initial steady increase in the peak current at 0.0 V over the first seven cycles is attributed to the double-layer charging contribution of the rhodium rather than palladium oxide stripping. At high cycle number the two reach a plateau where, once again, the charges correspond to those expected for high surface area $H_1$-e films of the two different metals. In this case dissolution of the palladium is less pronounced, presumably because the presence of the overlying $H_1$-e rhodium film slows the diffusion of soluble palladium species from the electrode surface.

This ability to deposit $H_1$-e layers in which pores interconnect is not restricted to palladium and rhodium films. In other experiments we have obtained similar results for combinations of platinum and rhodium and platinum and palladium, although in the latter case the voltammetry is harder to interpret because the oxide stripping peaks overlap. For example, Figure 13 shows

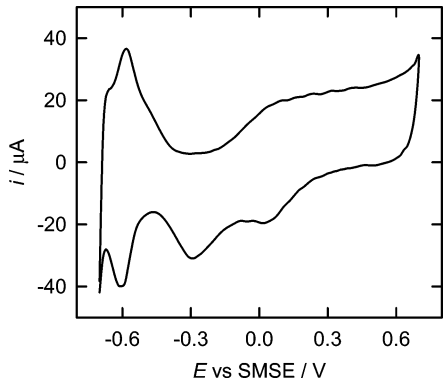


**Figure 13.** Cyclic voltammogram recorded at 100 mV/s in 1 M $H_2SO_4$ for a film with $H_1$-e Rh deposited on top of $H_1$-e Pt on a gold disk electrode (area 0.0079 $cm^2$). The charge passed to deposit each layer was 3.5 mC. The $H_1$-e platinum film was deposited from a template mixture containing 47 wt % $C_{16}EO_8$, 39 wt % water, 12 wt % $H_2PtCl_6$, and 2 wt % heptane. The film was soaked in water for 1 h prior to the measurement to remove the surfactant.

a voltammogram for a bilayer film prepared by depositing an $H_1$-e rhodium film on top of an $H_1$-e platinum film. The voltammogram shows a superposition of the voltammetry of the rhodium and platinum (compare Figures 5 and 13) with oxide stripping peaks for both rhodium and platinum clearly visible at −0.3 and +0.05 V, respectively, confirming that the upper rhodium film does not block access to the lower platinum film.

## Conclusions

We have shown that if we deposit one $H_1$-e on metal film on top of another from a plating mixture containing the same surfactant and concentration of cosolvent, the pores within the lower mesoporous film remain accessible and the electroactive surface area of the inner layer does not change as the outer layer is made thicker. By making time-dependent cyclic voltammetric measurements as the template surfactant leaves the pores of the bilayer structure, we have shown that the surface of the outer metal layer becomes electroactive first followed by the surface of the inner metal layer. On the basis of this result, we conclude that the pores in the outer and inner layers of the $H_1$-e film are continuous through the film so that the electrochemistry for the inner metal layer only appears once the surfactant has left the outer part of the pore. Our results show that the $H_1$ nanoporous structure shows alignment of the pores in the outer film by those in the inner layer. In other words the surfactant micelles in the plating mixture used to deposit the outer metal film align themselves at the surface of the electrode so that they align with the surfactant-filled pores in the first nanostructured film. This is not unreasonable since the micelles in the lyotropic liquid-crystalline phase are reasonably mobile and this type of arrangement may be expected to minimize the interfacial free energy for the system.

The fact that we can readily deposit $H_1$-e films in which the pores run continuously through the different metal layers in the structure opens up the possibility of making mesoporous multilayer structures which may have interesting catalytic or other properties and of preparing $H_1$-e metal films in which the outer surface is passivated or coated by a thin insulating layer formed from a different material. The results presented here also mean that we can use this approach to build up thick $H_1$-e films of a single metal. At present, a limitation on the deposition of thick $H_1$-e films is simply the time taken for the process because as deposition continues the current falls because all the metal ions near the electrode are consumed. In a normal aqueous plating bath mass transport by convection can be used to overcome this problem. For the lyotropic liquid-crystalline phases this is not possible because of their high viscosity. By depositing the $H_1$-e film in several stages, it should be possible to overcome this problem and still have continuity of the pores through the film, and hence a high surface area.

**Acknowledgment.** This work was supported in part by the EPSRC (Grant GR/M51284) and in part by a research studentship for J. M. from City Technology Ltd.

CM0210400